

**ICSO 2016**

**International Conference on Space Optics**

Biarritz, France

18–21 October 2016

*Edited by Bruno Cugny, Nikos Karafolas and Zoran Sodnik*



***Coherent photonic beamformer for a Ka-band phased array antenna receiver implemented in silicon photonic integrated circuit***

*V. C. Duarte*

*A. Pęczek*

*M. V. Drummond*

*R. N. Nogueira*

*et al.*



## COHERENT PHOTONIC BEAMFORMER FOR A KA-BAND PHASED ARRAY ANTENNA RECEIVER IMPLEMENTED IN SILICON PHOTONIC INTEGRATED CIRCUIT

V. C. Duarte<sup>1,2,3</sup>, A. Pęczek<sup>3</sup>, M. V. Drummond<sup>1</sup>, R. N. Nogueira<sup>1,4</sup>, G. Winzer<sup>3</sup>, D. Petousi<sup>3</sup> and L. Zimmermann<sup>3</sup>

<sup>1</sup>*Instituto de Telecomunicações, 3810-193, Aveiro, Portugal.*

<sup>2</sup>*Department of Physics, University of Aveiro, 3810-193, Aveiro, Portugal.*

<sup>3</sup>*IHP – Innovations for High Performance Microelectronics, 15236 Frankfurt (Oder), Germany.*

<sup>4</sup>*Watgrid Lda., 3810-193, Aveiro, Portugal.*

### I. INTRODUCTION

The generation of satellite communications with flexible and efficient transmission of radio signals requires a large number of low interfering beams and a maximum exploitation of the available frequency spectrum. In this context, the implementation of phased array antennas (PAA) working in Ka-band allows to fulfil such requirement and increase the overall capacity available in the desired bandwidth. Furthermore, the operation in the Ka-band allows a higher consumption of the bandwidth due data traffic, arriving to 100Gbps for the multibeam application [1]. To arrive to a target of a next generation of satellite payloads capacity (Tb/s) it is needed a multiple beam capability with multi-feed per beam. Since the capacity of the payloads are dependent on the available bandwidth, it implies the available bandwidth of each antenna element (AE) and also the bandwidth of the techniques and devices implemented to transmit/receive the data information. One of these techniques is the use of beamforming systems. The current radio-frequency (RF)-beamforming payloads suitable for the target capacity of Tb/s, would come with a high volume, complexity, power consumption and consequently a high cost to mass, especially when launching the satellite. Hence, a solution for the wanted Tb/s payloads would be the implementation of photonics in the system. This would be beneficial since the telecom payload capacity would increase and at the same time the power consumption would decrease. In addition some advantages like low loss, large bandwidth, immunity to electromagnetic interference and light weight would be present. With the implementation of the complementary metal-oxide-semiconductor (CMOS)-compatible silicon photonic integrated circuits (PICs), specifically tailored for space applications, the telecom satellite would be even less complex with a decreasing on the mass, volume and, consequently, on the launching costs.

BEACON - Photonics for telecom satellites [2] is a technology-intensive project that aims to provide the missing enabling technologies for the development of a new generation practical, low-cost and high capacity beamforming Tb/s payload system. BEACON technology will help enabling the sustained entry of photonics inside payloads, disrupting the capacity upgrade of multi-beam telecommunication satellite payloads, while at the same time leveraging the R&D investment to address next generation coherent intersatellite links with fully integrated and practical components. This project builds on the collaboration of different companies and research centers in order to develop high-speed GaAs electro-optic modulator arrays, radiation-hard optical amplifier arrays, and a multibeam silicon photonic integrated beamformer.

In traditional beamformer payloads, such as based on phase shifters, the system is squint-free only for a given target frequency. This drawback can be overcome with beamformer systems based on true time delay (TTD) lines. In a TTD beamforming system, the signals are effectively delayed ensuring that the phase shifts experienced by all frequencies are correct, thereby avoiding beam squinting.

In this paper we present the first experimental results of the photonic true-time delay beamforming system designed for a Ka-band phased array antenna receiver (27.5 – 30 GHz), proposed in [3], and developed within the scope of project BEACON. The proposed photonic beamforming system for a PAA receiver is based on tunable optical delay lines (TODLs) and on self-heterodyne coherent detection [3]. The TODLs have a simple, potentially fast tuning mechanism, thereby enabling dynamic TTD beamforming. Plus, the system offers maximum sensitivity, self-heterodyne coherent detection that enables phase noise cancellation, photonic RF phase shifting and also photonic RF frequency downconversion. The latter advantage is very important for relaxing the bandwidth of the electrical circuitry of the receiver. For the integration of the developed photonic beamforming in a PIC, different layouts with different kinds of phase shifters were designed and produced through the fabrication of complementary metal-oxide-semiconductor (CMOS)-compatible silicon photonic integrated circuits (PICs). Preliminary tests on-wafer for all types of phase shifters implemented in the system were performed and are presented in the paper.

## II. OPERATION PRINCIPLE

The beamformer [3], relies on simple tunable optical delay lines and also on self-heterodyne coherent detection, as depicted in **Fig. 1**. In the upper path, each antenna element produces a modulated optical signal, which is phase shifted by  $\beta$  and then delayed by a Mach-Zehnder delay interferometer with tunable coupling ratio (MZDI-TCR). The phase shifter  $\beta$  is required in a system with multiple AE to adjust the phase of each modulated optical signal, such that all signals add up with the correct phase. The MZDI-TCR allows varying the delay from 0 up to the delay of the interferometer. The adjustment of the frequency response of a MZDI-TCR requires at least two phase shifters, one for controlling the power coupling ratio between the arms of the MZDI-TCR,  $\phi$ , and another to center its frequency response,  $\gamma$ .

The frequency-shifted optical local oscillator (FSOLO) is generated in the lower path by modulating the input optical signal with an IQ modulator (IQM). The delayed optical signals are combined and then coherently detected by the frequency-shifted copy of the input laser source. Such self-heterodyne coherent detection allows achieving maximum sensitivity inherent to coherent detection, and also laser phase noise cancellation, photonic RF phase shifting and photonic RF frequency downconversion.

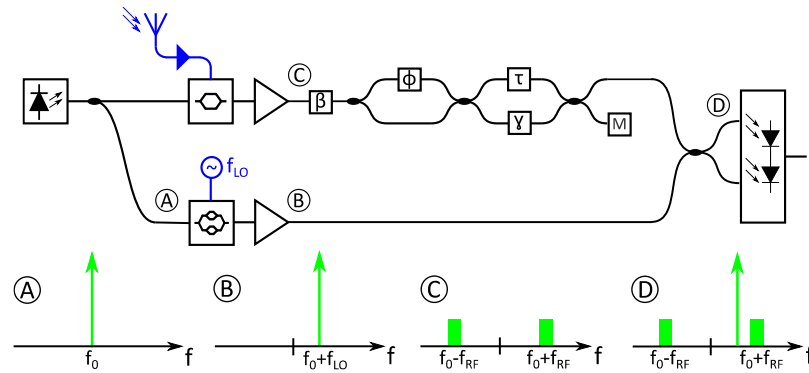


**Fig. 1.** Schematics of the photonic beamforming for a PAA.

To analyse the response of the TODL one needs to consider, the modulated optical signal after being phase shifted by  $\beta$ . Thus, the TODL output signals are given by

$$\begin{bmatrix} E_{\text{MZDI}}(f) \\ M(f) \end{bmatrix} = \frac{1}{2\sqrt{2}} \begin{bmatrix} e^{j\tau(f)}(e^{j\phi} - 1) - e^{j\gamma}(e^{j\phi} + 1) \\ je^{j\tau(f)}(e^{j\phi} - 1) + je^{j\gamma}(e^{j\phi} + 1) \end{bmatrix} \cdot E(f)e^{j\beta}, \quad (1)$$

where  $E_{\text{MZDI}}(f)$  is the delayed output optical signal,  $M(f)$  is the second output optical signal, which can be used for operation monitoring,  $\tau(f)$  is the transfer function of the optical delay line and  $E(f)e^{j\beta}$  is the input optical signal.

From (1), the amplitude and group delay responses of the TODL can be derived by setting  $\gamma = \pi/2$ , as the variation of  $\gamma$  only results in a displacement of the frequency response along the frequency. Such responses are given by

$$\|H(f)\|^2 = \frac{1}{2} (\sin(\phi) \cos(2\pi f\tau) + 1), \quad (2)$$

$$\tau_g(f) = \frac{\tau}{2} \left( \frac{\sin \phi \cos(2\pi f\tau) - \cos \phi + 1}{\sin \phi \cos(2\pi f\tau) + 1} \right). \quad (3)$$

**Fig. 2** shows the amplitude and group delay responses for a  $\gamma = 3\pi/2$  for different values of  $\phi$ . Both responses show a periodical behavior with a period of  $1/\tau$  and a group delay increasing with the phase shift. The optimum operation point is when the optic signal is aligned with the transfer function of the TODL. Thus, the amplitude and group delay responses needed to be centered in  $= 0, 1, 2, \dots$ . In addition, complementary angles have the same attenuation, where the maximum attenuation corresponds to 3 dB for  $0^\circ$  and  $180^\circ$ , and no attenuation of the signal for an angle of  $90^\circ$ .

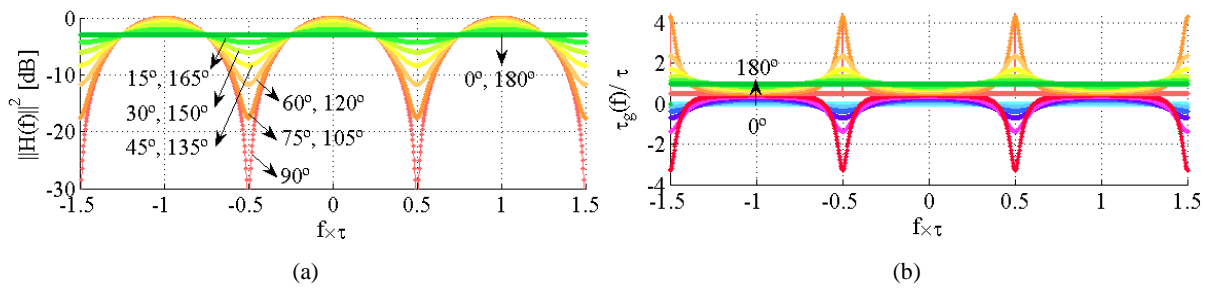


**Fig. 2.** Amplitude (a) and group delay (b) responses of the TODL for different values of  $\phi$  and  $\gamma = 3\pi/2$ .

The present photonic beamformer was design and produced in order to validate the concept in the future. Different phase shifters were then implemented and some preliminary tests were done.

### III. DEVICE DESIGN

Different layouts of the MZDI-TCR based beamformers, featuring different kinds of phase shifters were designed and produced with the fabrication of CMOS-compatible silicon PICs, specifically tailored for space applications based on the developed PDK SG25-PIC [4]. The aim of designing different layouts was assessing which kind of phase shifter would be more suitable for a robust operation. As such, in the MZDI-TCR waveguides was embedded thermo-optic phase shifters, injection of free carriers within a PIN junction and depletion of free carriers within a PN junction.

Thermal-optical phase-shifters work by placing a heater on top of a waveguide. The tuning is achieved by heating the waveguide, inducing a phase shift in the light that passes through it. This tuning affects the effective index of the optical mode of the waveguide, due to the heat. In these devices, the size and length restricts the length of the modulation region. Hence long structures are often needed. For longer structures there is an increase of the thermal resistance on the longitudinal heat flow. It is then required a larger change in the temperature and consequently leads to a lower speed and higher consumption [5]. Carrier injection phase-shifters are based on PIN diodes. When the PIN diode is forward biased, the electrons and holes are injected to the intrinsic region, where the waveguide is embedded. This leads to a change in the refractive index and in the phase of the signal. These structures allows to have a large modulation efficiency of the phase-shifters due to its high capacitance. On the other hand, carrier depletion phase-shifters are based in reverse biased PN diodes. Hence, the waveguide is embedded upon the PN junctions and, when reverse biased, the waveguide experience a reduction of the free carriers. This leads to a low capacitance, resulting in a low-modulation efficiency, however with no static current consumption, which is an important feature [6], [7]. Comparing the three phase shifters, carrier injection and depletion phase shifters have the advantage of being faster than thermo-optic phase shifters, less power consuming, although producing a higher attenuation of the signal than thermal-optical phase shifters. However, the speed of the thermal-optic can be increased for small structures. In addition, depletion phase-shifters enable zero current consumption, at the expense of a larger footprint, comparing with an injection phase shifters that allow to obtain a large phase-shifter modulation efficiency.

In **Fig. 3** is shown the scheme of the basic beamforming system layout of the designed and fabricated PICs. The beamformer is composed by an input optical splitter with tunable coupling ratio, in which are embedded two phase-shifters,  $\phi_1$  and  $\phi_2$ , and two thermo-optic phase shifters,  $H_1$  and  $H_2$ , with symmetric arms. The phase-shifters  $\phi_1$  and  $\phi_2$  are the ones suffering the changes in the layout between thermo-optic, injection and depletion phase-shifters. In addition the thermo-optic phase shifters,  $H_1$  and  $H_2$ , are present to allow a fine adjustment of the phase if needed. The MZDI that follows has a coil-shaped optical delay line with a delay of 50 ps,  $\tau$  and  $H_3$ , and two carrier-injection phase shifters in each arm,  $\gamma_1$  and  $\gamma_2$ , with 500 $\mu$ m and 300 $\mu$ m long, respectively. The carrier-injection phase shifter that follows the optical delay line is shorter than the one of the other arm so that the loss difference between the arms of the MZI is minimized and the same phase-shift can be achieved. Furthermore, the PIC also offers the possibility of combining the optical local oscillator (OLO) to the delayed optical signal as observed in the scheme.

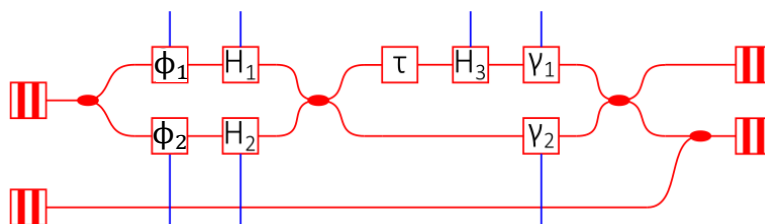


Fig. 3. Scheme of the basic structure of the PICs.

In Fig. 4 is shown the different variations of the beamforming system layout. As observed in Fig. 4 (a) the design of the input optical splitter with tunable coupling ratio only contains the thermo-optic phase shifters,  $H_1$  and  $H_2$ , with 2 mm long each one. The second design, Fig. 4 (b),  $\phi_1$  and  $\phi_2$  corresponds to a MZDI with a 1mm length carrier-injection phase-shifter and also a thermo-optic phase shifter in each arm,  $H_1$  and  $H_2$ , with 1.5 mm. The design shown in Fig. 4 (c) has in the first MZDI, a 5 mm long depletion high-speed MZM, also including two thermo-optic phase shifters with 1.5 mm length,  $H_1$  and  $H_2$ , for the fine adjustment of the phase. As observed in Fig. 4, the second MZDI shows the same design with the same structures for all of the three layouts.

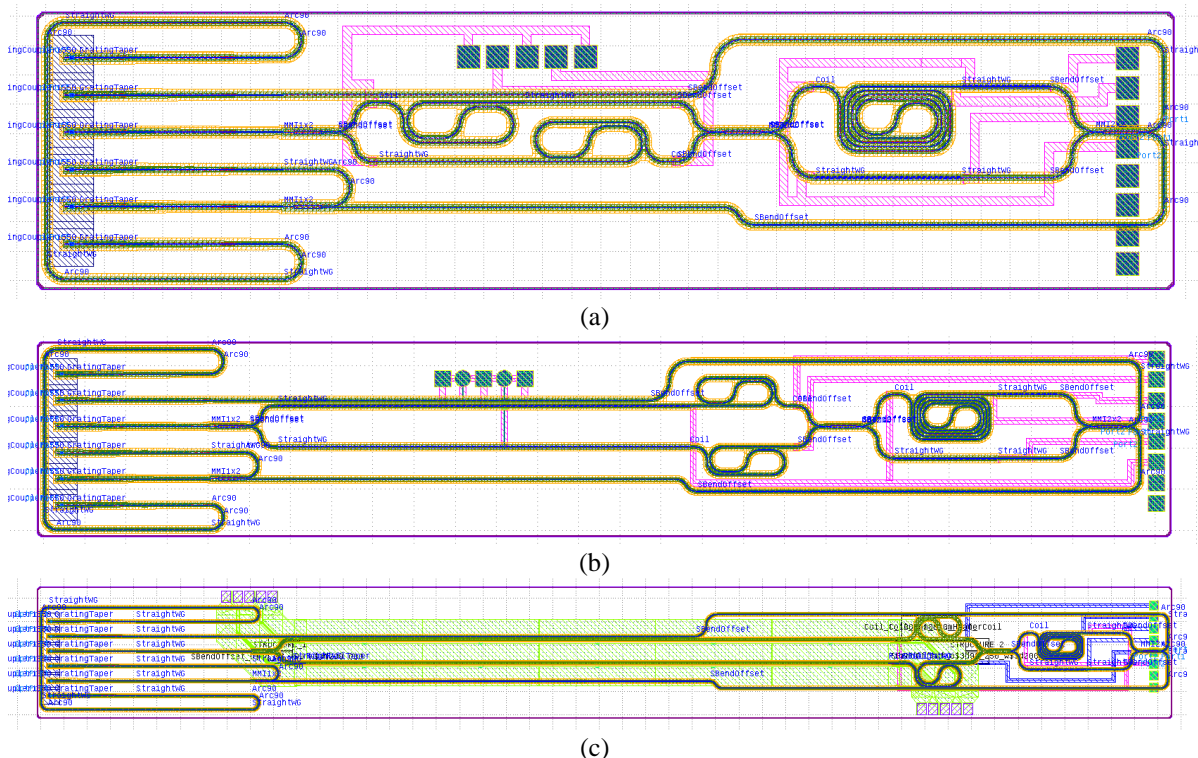


Fig. 4. Layout designs of the proposed photonic beamformer composed by: (a) thermo-optical phase-shifters, (b) carrier injection phase-shifters, (c) depletion phase-shifters.

These structures are typically used for high-speed electro-optic modulation, and, to the best of our knowledge, have never been used in integrated microwave photonics applications. Furthermore, the designs implemented in BEACON's PICs are also new which implies a detailed characterization of such system. Therefore, to start, the first preliminary tests in the MZDI's phase shifters were done and are shown.

#### IV. CHARACTERIZATION RESULTS

For the correct operation of the beamforming system shown in Fig. 1 (a), the phase-shifter  $\phi$  has to arrive to a phase shift of  $\pi$ , while  $\gamma$  needs a phase-shift of  $2\pi$ . However, the fabricated PIC only contains the beamformer, as shown in Fig. 3. Since the phase shifter  $\beta$  (Fig. 1 (a)) is not present, the PIC to work properly, needs a phase shift  $\phi$  and  $\gamma$  of  $2\pi$ .

The amplitude response of the beamformer structure, when biasing a phase-shifter, will be the characteristic response of an interferometer. As such, by knowing frequency variation of the interferometer with the applied voltage and the free spectral range, one can extract the dependence of the phase shift with the input voltage. The results of the phase-shift for the different applied voltages in the three types of phase-shifters  $\phi_1$ , and the response of both phase shifters  $\gamma_1$  and  $\gamma_2$  are presented in **Fig. 5** (a) and (b), respectively. Since  $\phi_2$  was doped and fabricated in order to be symmetric to  $\phi_1$ , the performance is basically the same, as such is not presented. Its presence in the MZDI has the aim to equalize the attenuation in both arms allowing to obtain a higher extinction ratio.

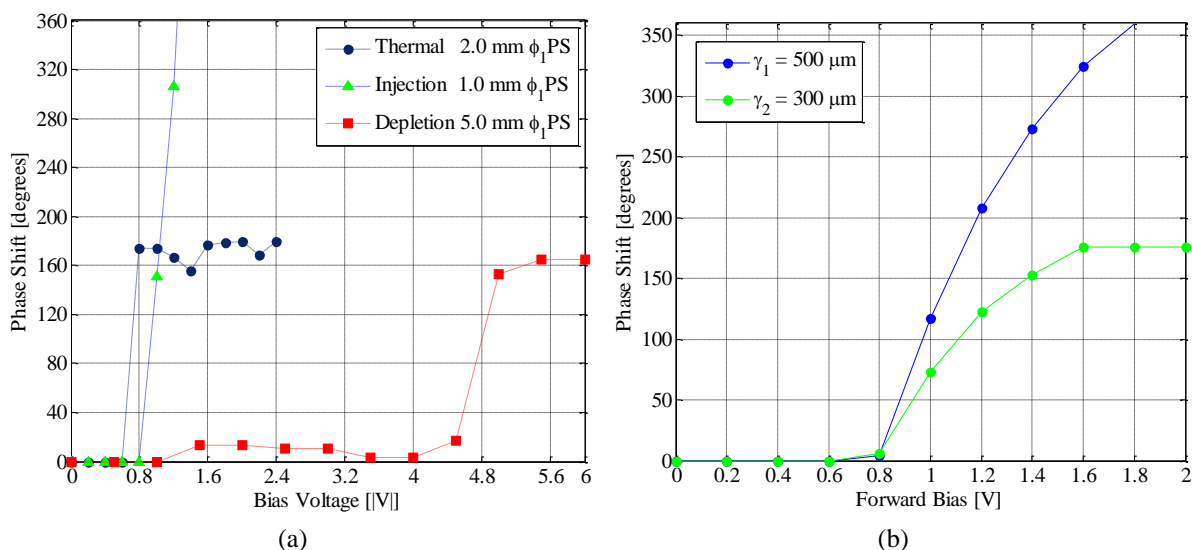


**Fig. 5.** Results of the phase shift with the increasing of the applied voltage for the different types of phase-shifters  $\phi_1$  (a) and phase shifters  $\gamma_1$  and  $\gamma_2$  (b).

As observed in **Fig. 5** (a) it is presented the phase shift for each type of  $\phi_1$  phase shifter when biased with different voltages. The thermal phase-shifter showed an increase of the phase shift with the voltage until  $\pi$ , observing after a saturation of the phase-shifter junction. This phase-shifter was also very slow to stabilizing the phase-shift, since it has to be heated, compared with carrier-based modulators. The carrier injection type was forward biased, achieving a  $2\pi$  phase shifter for 1.2 V and a current consumption of 15.7 mA. On the other hand the depletion phase shifter was reverse biased and achieved only a  $\pi$  for 5.5 V and no current consumption, being after observed the saturation of the carriers in the junction. Regarding **Fig. 5** (b) with both injection type modulators embedded in the second MZDI,  $\gamma_1$  and  $\gamma_2$ , it is observed that the  $500 \mu\text{m}$  carrier injection phase-shifter allows a phase-shift until  $2\pi$  when biased with 1.8 V. For a  $300 \mu\text{m}$  carrier injection-phase shifter, the maximum phase shift was  $\pi$  until we observe a saturation of the carriers in the N junction after 1.6 V. With the phase-shift achieved in both of the arms it is possible to bias both in other to achieve the required phase shift and at the same time balance the attenuation suffered by the injection of the carriers in the junctions. This will allow again, to achieve a better extinction ratio, important for the performance of the system. In addition the results are also in accordance with the ones obtained in the **Fig. 5** (a), where the 1 mm injection type modulator with the same PiN doping as the  $500 \mu\text{m}$  and  $300 \mu\text{m}$ , shows a phase shift of  $2\pi$  for 1.2 V and for  $500 \mu\text{m}$  was needed 1.8 V. In the case of the  $300 \mu\text{m}$  long it only achieved  $\pi$  phase shift for 1.6 V.

In order to evaluate the performance of the phase-shift  $\phi_1$  tuning also the heater  $H_1$ , different applied voltages were applied for the injection type, resulting in the graphic in **Fig. 6**.

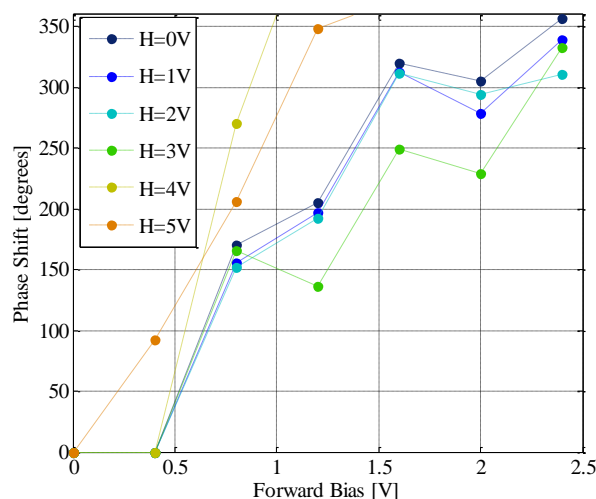


**Fig. 6.** Variation of the phase shift  $\phi_1$  with the applied bias for the carrier injection phase shifter  $\phi_1$  when applied different voltages to the heater  $H_1$ .

As observed in **Fig. 6** the phase shifter  $\phi_1$  behaves in a similar way when the heater  $H_1$  is biased until 2 V, with 3 V it is observed a degradation of the performance. However, when the heater is biased with 4 to 5 V the performance increases and the voltage needed to achieve a  $2\pi$  phase shift is 1 V. Since with the increasing of the bias voltage of the heaters, the phase-shift should increase, the behavior shown for 3V is probably a problem of temperature stabilization.

However, since these results are only derived from preliminary tests, more studies about the phase-shifters must be made, in this case, already embedded in a printed circuit board (PCB). This will allow to correctly operate one TODL, and to achieve a target transfer function or delay, by carefully tune its seven phase shifters. As such, an adaptive algorithm [8] which analyses the output signal of the system and adjusts the voltages until the target delay is achieved was developed. As only minimal characterization is required, three simple preliminary tests should be done to each TODL. Hence, these preliminary tests and the characterization of the phase shifters provided not only a first impression on the performance of the PIC samples, but will also provide valuable parameters that will be fed to the control algorithm for a correctly operation.

## V. CONCLUSION

The preliminary tests of the three types of phase shifters: thermal-optic, carrier injection and depletion; embedded in the MZDIs were performed. Regarding the phase shifter  $\phi_1$  present in the first MZDI, the injection type showed the highest phase-shift,  $2\pi$ , for a current consumption of 15.7 mA. In the case of thermal and depletion type, only a  $\pi$  phase shift was achieved for 0.8 V and 5.5 V, respectively, however the second with no current consumption. In respect to the injection phase shifters embedded in the second MZDI,  $\gamma_1$  and  $\gamma_2$ , with 500  $\mu\text{m}$  and 300  $\mu\text{m}$  long, the first show a phase-shift of  $2\pi$  when achieving 1.8 V and the second a phase-shift of  $\pi$  for a bias voltage of 1.6 V. By comparing the different results a first indication on the phase shifters of the first MZDI better suited for BEACON's applications might be the depletion type due to the no current consumption. However, for the beamformer PIC system, the better suited is the injection type, since it allows to obtain a  $2\pi$  phase-shift. Furthermore, in the future work, the test results will also be used for validating curves obtained by simulation regarding the dependences of the phase shift with the input voltage. Plus, besides this preliminary tests, tests on PCB will be made in order to correctly operate the TODL.

## ACKNOWLEDGEMENTS

This work is co-funded by FCT/MEC through national funds and when applicable co-funded by FEDER – PT2020 partnership agreement under the project UID/EEA/50008/2013 and also supported by the European Commission through the project BEACON (FP7-SPACE-2013-1-607401).

REFERENCES

- [1] P. Inigo, O. Vidal, B. Roy, E. Albery, N. Metzger, D. Galinier, J. Anzalchi, G. Huggins, and S. Stirland, "Review of terabit/s satellite, the next generation of HTS systems," *2014 7th Advanced Satellite Multimedia Systems Conference and the 13th Signal Processing for Space Communications Workshop (ASMS/SPSC)*. pp. 318–322, 2014.
- [2] "BEACON, photonics for telecom satellites." [Online]. Available: <http://www.space-beacon.eu/>. [Accessed: 31-Aug-2016].
- [3] V. C. Duarte, M. V Drummond, and R. N. Nogueira, "Photonic True-Time-Delay Beamformer for a Phased Array Antenna Receiver based on Self-Heterodyne Detection," *Unpublished*, 2016.
- [4] "Low-Volume & Multi-Project Service." [Online]. Available: <https://www.ihp-microelectronics.com/de/services/mpw-prototyping/sigec-bicmos-technologies.html>. [Accessed: 31-Aug-2016].
- [5] A. Malik, S. Dwivedi, L. Van Landschoot, M. Muneeb, Y. Shimura, G. Lepage, J. Van Campenhout, W. Vanherle, T. Van Opstal, R. Loo, and G. Roelkens, "Ge-on-Si and Ge-on-SOI thermo-optic phase shifters for the mid-infrared," *Opt. Express*, vol. 22, no. 23, pp. 28479–28488, 2014.
- [6] L. Vivien, L. P. Eds, A. Ram, D. Marris-morini, R. A. Soref, D. J. Thomson, G. T. Reed, R. K. Schaevitz, D. A. B. Miller, T. Kerr, F. K. Effects, S. L. Sources, A. Anopchenko, A. Prokofiev, I. N. Yassievich, S. Ossicini, L. Tsybeskov, D. J. Lockwood, S. Saeed, T. Gregorkiewicz, M. Wojdak, J. Liu, A. Meldrum, L. Emission, S. Nanostructures, M. Notomi, K. Nozaki, S. Matsuo, T. Baba, O. Boyraz, X. Sang, M. Cazzanelli, Y. Huang, T. Lei, S. Feng, A. Sayarath, J. Song, W. Bogaerts, D. Vermeulen, K. Yamada, T. Tsuchizawa, H. Fukuda, C. Koos, J. Pfeifle, J. H. Schmid, P. Cheben, P. J. Bock, A. P. Knights, S. Photovoltaics, M. Tucci, M. Izzi, R. Kopecek, M. Mccann, A. Le Donne, S. Binetti, S. Huang, G. Conibeer, D. Xu, S. Janz, A. Densmore, A. Delâge, R. C. Bailey, A. T. Heiniger, Q. Lin, P. M. Fauchet, Q. Wang, Y. Chao, T. Pinguet, J. Fedeli, F. L. Royo, J. Michel, S. J. Koester, X. Wang, M. W. Geis, S. J. Spector, M. E. Grein, J. U. Yoon, T. M. Lyszczarz, N. Feng, E. Kasper, M. Oehme, M. Bauer, M. Kittler, M. Reiche, O. Nakatsuka, and S. Zaima, "Handbook of Silicon Photonics." pp. 479–552, 2013.
- [7] T. Baba, S. Akiyama, M. Imai, N. Hirayama, H. Takahashi, Y. Noguchi, T. Horikawa, and T. Usuki, "50-Gb/s ring-resonator-based silicon modulator," *Opt. Express*, vol. 21, no. 10, pp. 11869–11876, 2013.
- [8] V. C. Duarte, M. V Drummond, and R. N. Nogueira, "Coherent photonic true-time-delay beamforming system for a phased array antenna receiver," *2016 18th International Conference on Transparent Optical Networks (ICTON)*. pp. 1–5, 2016.